

SHOCK WAVE PROPAGATION AND NASTRAN LINEAR ALGORITHMS

Dr. M.M. Moharir
Senior Engineering Specialist
General Dynamics Space Systems Division
San Diego, California 92138

Presented at
MSC/NASTRAN Users Conference
Pasadena, California
March 20-21, 1986

Abstract

A study is conducted to investigate usage of NASTRAN as a viable tool to analyze shock wave propagation through solids. Fundamental variables such as velocity of sound, maximum length of unreflected travel, duration of pulse, finite-element dimensions, analysis time step, fundamental period of the structure, etc. are identified and their mutual relationship established for the proper solution in NASTRAN environment. Modal and direct transient algorithms with superelements are covered for the impulse and the enforced motion shock waves.

1. INTRODUCTION

A study is conducted to investigate use of NASTRAN as a tool to analyze shock wave propagation through solids. The work is limited to the linear transient algorithms. Explicit and implicit theoretical formulations are discussed. Dimensional analysis is performed on the parameters involved in the wave propagation phenomenon and the modeling technique of NASTRAN.

A general procedure circumventing limitations in NASTRAN algorithm is reported for the practical structures. Lumped mass and coupled mass discretization procedures are one of the study parameters in the NASTRAN model. The solution sequences include SOL 63 Mode Data Base, SOL 27 and 69 Direct Transient Response, and SOL 31 and 72 Modal Transient Response with and without superelements.

2. SHOCK WAVE PHENOMENON

When an instantaneous disturbance is applied to a structure through a generalized force or a kinematic parameter, the disturbance travels through the structure, deforming it and thus generating the stress tran-

sients. In the explicit mathematical formulation of wave mechanics, the initial disturbance is regarded as composed of an infinite number of sine-wave components of all wavelengths but of the same amplitude. This Fourier-type representation is solved for the coefficients, considering the boundary conditions of the structure and the defined input disturbance at the starting time ($t=0$). The stress generated is a function of the velocity of sound in the structural media.

The NASTRAN solutions are based on the classical structural dynamics theories of modal superposition or direct transient analyses. The two methods give identical results at small incremental time steps (Reference 6). Terms similar to the velocity of sound are embedded in the eigenvalue solutions of the classical approach. A finite-element grid and the location of mass points must be selected by the user in the NASTRAN model. This finite-element discretization, whether based on lumped mass or the coupled mass method, is a major source of difference in the analytical results compared to the explicit wave mechanics formulation. The subject is discussed in details in Section 4.1.2.1.

Note at this stage that the current study is for the wave propagation through solids under linear conditions. It does not account for material or geometric nonlinearities nor for any distortion in the finite-element section. Therefore, the details of Lagrange and Euler formulations are not discussed. However, it does account for the transverse wave propagation when the masses have all the six degrees of freedom. To obtain a 3D-wave effect, the rotational degrees of freedom may be omitted in the NASTRAN model.

3. SELECTION OF PARAMETERS

The list of important parameters involved in the study of wave propagation phenomenon using NASTRAN, is as follows:

- Δt = Analysis time step
- V_s = Velocity of sound in the structural media
- L_r = Largest dimension of the structure along which the sound wave travels before reflection
- L_e = Length of the finite element in the direction of wave propagation. If wave is not unidirectional then L_e is minimum of the individual directions.
- t_p = Duration of the pulse (Section 4.4)
- T_d = Total duration of the analysis
- T_f = Fundamental period of the structure i.e. $1/F_{\min}$ where F_{\min} is the lowest nonzero frequency.

Basically, there are three considerations:

- (i) Theory of Wave Mechanics,
- (ii) Finite Element Analysis, and
- (iii) NASTRAN Algorithms

which impose the following constraints on the final selection of the study parameters.

- (a) $\Delta t \leq L_e/V_s$

This restriction helps to superpose the incoming and reflecting shock waves at the boundary elements. Violation may result in the lower magnitude of stress at the reflection points.

(b) $\Delta t < T_{fmin}/10$ (Reference 4)

Violation may result in neglecting the effect of higher modes. Smaller Δt is required for the closely spaced modes.

(c) $t_p < T_f$

This is subjected to the definition of input shock.

(d) $t_p > 5\Delta t$ when the input function is a transient force, $t_p > 7\Delta t$ when the input function is an imposed motion.

This is to satisfy the three-point-averaging scheme of NASTRAN at the ascending and descending of the input function. If only the latter part of the function is present, multipliers 3 and 5 may be used in place of 5 and 7, respectively.

(e) L_e should be small enough to satisfy the usual requirements of finite element analysis. These requirements differ from element to element (Reference 5).

(f) $L_e < t_p V_s/7$

This restriction comes from the implementation of wave mechanics principles in NASTRAN environment. Violation results in wrong amplitudes at generation, propagation, and reflection.

(g) $T_d > T_f$

This is to account for the basic resonance conditions.

(h) $T_d > 4(L_r/V_s)$

This is to catch the maxima at the rereflected and reflected waves. After this time, the waves generally die down.

If the input shock function is predefined through experimentation or analytical method (Section 4.2.2), the corresponding t_p value will take precedence. Some of the Δt requirements are very stringent, resulting in the analysis time step in the order of 0.01 microsecond. A variable time step is suggested in Section 4.1.2.5. A larger value should be considered past the approximate times t_p and $N(L_r/V_s)$, especially when modal transient solution is used. Value of the constant N depends on t_p . In other words, the maximum stress can occur at any of the reflected waves, depending on the input forcing function.

3.1 SELECTION PROCEDURES — The selection procedure depends on the area of application, which is divided into two categories:

- (1) When an input function is predefined. In that situation, the user is to select the finite-element size from the minimum of item (e) and item (f). This case is encountered in blast analysis and similar problems. The typical t_p values are discussed in Section 4.4.
- (2) When the input function is to be defined by the user (e.g. a case of a linear impact analysis similar to Hopkinson's experiment). One should take advantage of a large finite-element size by using the item (e) and then selecting t_p by item (f).

The subsequent value of analysis time step comes from the minimum of items (a), (b), and (d). The fundamental period of the structure is not known until the execution of first run. It may necessitate some modifications in the selected data.

4. NASTRAN TEST CASES

The test cases are divided into two categories:

- (i) Shock wave generated by impulse,
- (ii) Wave propagation study of Hopkinson's experiment.

This helps to test the NASTRAN transient analysis algorithms under sudden pressure and enforced motions separately. The test data is varied to conduct the parametric studies of Section 3.

4.1 STRETCHED CANTILEVER

4.1.1 Wave Mechanics Formulation — This case is discussed in detail in Reference 2. A prismatic bar is fixed at one end and free at the other. It is initially stretched by a force P, giving an initial stretch condition

$$U_0(x) = PX/AE \quad (1)$$

The natural frequencies of the bar under longitudinal vibrations (Figure 1) are:

$$f_n = \frac{(2n-1)\pi}{2L} \sqrt{\frac{E}{\rho}} \quad (2)$$

The bar is let free after the initial condition (1). The stress transient is given by:

$$= \frac{4P}{\pi A} \sum_{n=1,2,3}^{\infty} \frac{(-1)^{n-1}}{(2n-1)} \cos \frac{(2n-1)\pi x}{2} \cos f_n t \quad (3)$$

NASTRAN stress time-history at each of the fixed, middle, and free sections of the cantilever will be compared with the one of Equation 3.

4.1.2 NASATRAN Test Data — To start with, data is selected to test the numerical stability of the NASTRAN algorithm under small input quantities. The analysis time step may go as low as 0.01 microsecond and the element length of 0.002 ft. To keep the computer run time (CPU) down, the following variables are selected:

$$E = \text{Young's Modulus} = 30 \times 10^6 \text{ psi}$$

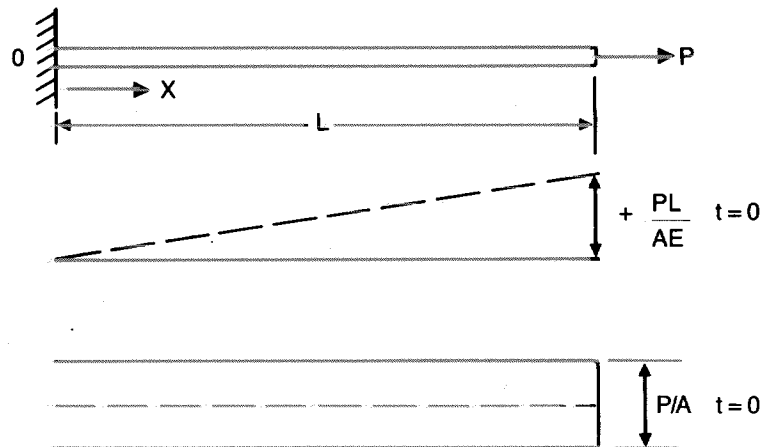


Figure 1. Longitudinal vibrations of a prismatic bar.

$$\begin{aligned} \rho &= \text{Mass density} = 15.093 \text{ lb-mass/cu ft} \\ V_s &= \sqrt{E/\rho} = 16,918 \text{ ft/sec} \\ L_r &= \text{Length } L \text{ in Figure 1} = 0.1 \text{ ft} \\ L_e &= 0.1/50 = 0.002 \text{ ft} \\ T_t &= \text{Time of travel of sound wave before reflection} \\ &= 0.1/16918 = 5.91 \text{ microseconds} \\ A &= \text{Cross sectional area of the rod} = 0.1 \text{ ft}^2 \\ P &= 1.0 \times 10^8 \text{ lb} \end{aligned}$$

The material properties and the speed of sound used here are typical of steel structures.

From this data it is seen that item (f) on Section 3 is ignored. This is a special test case in which the shock wave is automatically generated by the initial condition of Equation 1 and the sudden release of the stretching force. It has resulted in economic runs, since the element length is 0.002 ft instead of 0.00012 ft, during all the parametric studies except of L_e versus t_p variation. The latter variation is carried out in Sections 4.2 and 4.3. However, the element size L_e must be less than $(t_p V_s/7)$ in absence of the initial condition similar to Equation 1.

4.1.2.1 Run SH0K6 — The numerical data listed above is used in the NASTRAN run SH0K6. Analysis time step is 0.01 microsecond. Total number of time steps is 1,500. Initial tensile displacements, ranging from zero to PL/AE values, are provided on the "TIC" Bulkdata cards. The input forcing function which relieves the initial tensile displacements is drawn in Figure 2. Negative stresses in the graphs of Figures 3 through 19 are treated as tension.

The masses are lumped at the grid points. Direct transient solution SOL 27 is used. The stress transients are plotted for the fixed edge (element 50), central section (element 25) and, free edge (element 1) as shown in Figures 3, 4, and 5, respectively. Close inspection of these graphs helps validate the following theoretical conclusions:

- (i) At the reflecting edge (element 50), stress is P/A till $L/V_s = 5.9$ microseconds then reverses to $-P/A$ illustrated by the graph in Figure 3.
- (ii) At mid span, the stress is P/A till $L/2V_s = 2.95$ microseconds, then goes to zero till $3L/2V_s = 8.87$ microseconds. The stress reverses to $-P/A$ up to $5L/2V_s = 14.8$ microseconds, as seen from the graph of Figure 4.

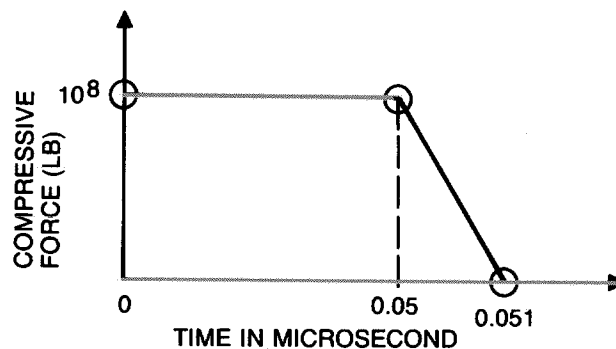


Figure 2. Input forcing function.

(iii) At the free end, stress at $t=0$ is P/A and immediately goes to zero. Then it starts to reverse at $2L/V_s$ = 11.8 microseconds as shown in Figure 5.

From these graphs it is clear that the NASTRAN values oscillate at the mean predicted by the Wave mechanics Theory. These oscillations are not the same as the "ringing" effect observed during a numerical instability.

The oscillations are the effect of discretization. The finer the finite-element mesh, the larger the number of oscillation loops. NASTRAN generates the eigenvalues (RUN SHOK1) close to those given by Equation 2, in addition to the fractions thereof. These extra frequencies add to the resonating conditions, thus overshooting (in both positive and negative directions) around the mean theoretical value. The effect decays with the passage of time, (t), because of the increasing dominance of t in the function $(t-T_{fn})$.

The graph of Figure 5 indicates that when there is a fast reversal of stresses (e.g. from $3L/2V_s$ to $2L/V_s$ to $5L/2V_s$), NASTRAN fails to capture the local peak at the central time ($2L/V_s$). This is because of the three-point-averaging scheme of NASTRAN. Since the absolute maximum at the section does not occur at such reversal, the design stress is still acceptable.

4.1.2.2 Run SHOK1R2 — A larger analysis time step is used ($\Delta t = 0.1$ microsecond). This is in violation of items (a) and (b) of Section 3. It also results in a larger value of t_p not being acceptable by items (c) and (d).

SHOK1R2 results fail to correlate theoretical values.

4.1.2.3 Run SHOK2B — This run is an attempt to check if any effect of lumped mass system has filtered into the results of the run SHOK6. The run SHOK2B uses the coupled mass algorithm of NASTRAN. The results are almost identical to those of SHOK6. The three validation items of Section 4.1.2.1 are correctly duplicated. The only difference is the number of oscillating loops around the mean theoretical value. This is expected because of the changes in the eigenvalue computations of the lumped mass and the coupled mass methods of NASTRAN.

4.1.2.4 Run SH0E2A — In this test case, the element length is increased almost six times, from 0.002 ft to 0.0125 ft. The results duplicate the theoretical values of Section 4.1.2.1. Since the fundamental frequencies are somewhat different between the two models, the number of oscillating loops differs. However, the mean values remain the same.

With the increase in element size, one may tend to increase the analysis time step Δt by the item (a) of Section 3. This is still acceptable so long as the items (b), (c), and (d) are also satisfied. It is obvious that the element size should be small enough to account for the requirements of finite-element analysis, which responds to the dynamic behavior of the structure.

4.1.2.5 Run SH0E2B — This run uses a variable time step past t_p (0.05 microsecond) and $2(L_2/V_s)$ approximately. The run SH0E2A is modified to give 0.05 microsecond time step after 10 microseconds. Thus, SH0E2B uses 1,000 steps of 0.01 microsecond and 100 steps of 0.05 microsecond. The results are identical to those of SH0E2A, even beyond 10 microseconds. Saving in CPU time is about 20 percent.

4.1.2.6 Runs SHOK5 and SHOL5 — These runs establish the dimensional analysis validity of the current discussion of NASTRAN results. Thus, the constraints of Section 3 for the selection of input parameters are

independent of the size of the structure used. Smaller dimensions of SHOK5 are to check that no numerical instability occurs even at very small time steps (0.01 microsecond) and element length (0.002 ft). The structure in run SHOL5 is exactly 100 times larger but of the same material; i.e., steel. This will make the time ratio also 1:100 for SHOK5 and SHOL5 runs.

The study parameters are listed in Table 1. Number of time steps is limited to 500 to save CPU, also it is sufficient for the comparative study.

NASTRAN graphs of Figures 6, 7, and 8 are for the stress transients at fixed end (element 50), mid section (element 25) and the free end (element 1) in the run SHOK5. The corresponding graphs of the run SHOL5 are given in Figures 9, 10, and 11.

These respective graphs of the model and the prototype (1:100 ratio) fit exactly one on the top of the other. Also, they agree with the theoretical validations of Section 4.1.2.1.

Table 1. Dimensional analysis study of the shock wave parameters.

S.N.	Nastran input	Run SHOK5 (model)	Run SHOL5 (prototype)
1	Length of the structure, $L = L_\gamma$	0.1 ft	10 ft
2	Length of finite element, L_θ	0.002 ft	0.2 ft
3	Analysis time step Δt	0.01 microsec	1 microsec
4	Analysis duration T_d (500 steps each)	5 microsec	500 microsec
5	Lumped mass at each of 50 grids, (except end grids)	0.023148 lb-mass	2.3148 lb-mass
6	Plateau time of input function, t_p	0.05 microsec	5 microsec

4.2 WAVE PROPAGATION IN HOPKINSON'S EXPERIMENT

4.2.1 Experimental Setup — A circular mass pierced by a hole is threaded on a wire and can be dropped from a known height. It strikes a clamp attached to the bottom of the wire (Figure 12).

Using different masses dropped from different heights, it can be shown that the minimum height from which a mass has to be dropped to break the wire is nearly independent of the magnitude of the mass. Also, the height of the fall can be adjusted so that the wire may break either at the bottom or at the top end.

When the mass hits the clamp, a velocity transient is applied to the bottom end of the wire. It generates a tensile stress wave, traveling upward with the speed of sound. If the yield stress of the wire is less than $V_s V_o \rho$, the wire breaks at the bottom. Otherwise, the tensile wave goes to the fixed end and reflects back with twice the amplitude ($2\rho V_s V_o$). Now, the wire has a possibility of breaking at the top. Next, when the wave reaches the bottom, it slows down the clamp and the mass. The subsequent reflection from the top generates the stress $2.13\rho V_s V_o$ at the point of reflection (Ref. 1).

4.2.2 NASTRAN Model — Run SHOK6 described in Section 4.1.2 is used as a model to duplicate the results of Hopkinson's experiment. Data base is generated in Solution 63 and restart is done in Solution 72 by changing the velocity input function in each of the runs of the next section. Also, in accordance with the linear dynamic analysis, the required amplitude of the initial tensile wave created at the free end can be slightly greater than $\rho V_s V_o$ so that the actual stress generated by the incoming tensile wave at the fixed end is $\rho V_s V_o$. This behavior depends on the vibrational characteristics of the wire. The tensile wave may

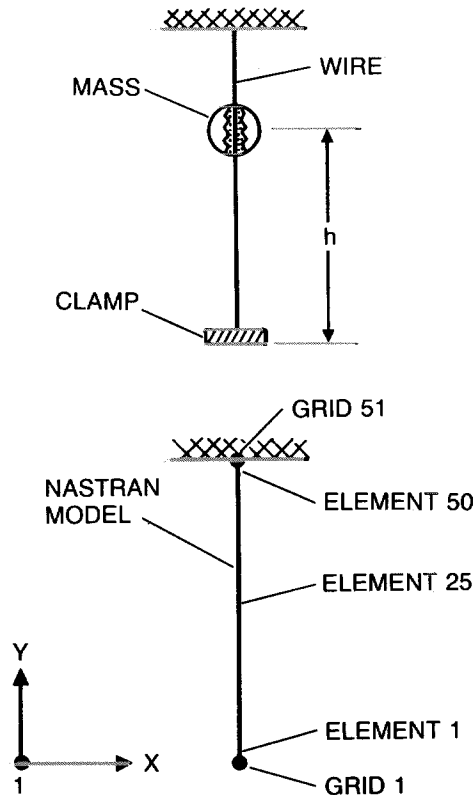


Figure 12. Experimental setup.

experience a decaying amplitude during its upward journey from the free end to the fixed one. As mentioned in Section 4.1.2.1, negative stresses in the graphs of Figures 3 through 13 are treated as tension.

4.2.3 Input Forcing Function of NASTRAN — One of the major considerations in this experiment is the time at which the mass decelerates sufficiently (Ref. 1) after hitting the clamp. In the original experiment, this time was long enough for the head of the stress wave to travel the length of wire several times. Damping of the mass-clamp assembly will affect the rate of deceleration.

Hopkinson could change the damping force by varying the size of the mass. No data is available on the actual damping forces generated under these conditions. The difficulty can be overcome by adjusting the value of t_p in the NASTRAN input. When the mass decelerates faster, t_p is smaller. The value of t_p should not be too large otherwise item (c) of Section 3 will be violated. Also, t_p should not be too small to affect the stress-sustaining capacity of the original experiment which reports the data (Ref. 1) of the reflected and the rereflected waves.

The following test runs illustrate the effect of variation in t_p on sustaining the stress wave observed in the experiment.

Run WAVE7R5 — $t_p = 0.05$ microsecond, $\Delta t = 0.01$ microsecond. This is in violation of item (d) of Section 3 ($t_p > 7 \Delta t$). The stress wave of proper amplitude is not generated even at the free end (Figure 13).

Run WAVE7R6 — $t_p = 0.5$ microsecond, $\Delta t = 0.01$ microsecond. This generates correct stress wave $\rho V_s V_0 = 647,984$ lb/sq ft. The wave reaches the middle section and the fixed end at the expected timings

of about $L/2V_s$ and $L/V_s (= 5.91)$ microseconds. However, t_p is too small to maintain the reflecting wave. (Figures 14, 15, and 16). In other words, the finite element grid is too coarse compared to the one demanded by item (f).

Run WAV7R10 — $t_p = 5$ microsecond, $\Delta t = 0.01$ microsecond. This run generates a shock wave similar to the Hopkinson's experiment. The wave of amplitude $V_s V_o \rho$ reaches the fixed end at L/V_s time, then almost immediately reflects with $2\rho V_s V_o$ magnitude and then reflects at $3L/V_s$ with $2.1 \rho V_s V_o$ approximate values. The graph in Figure 17 illustrates this wave propagation.

Thus, the velocity input function of Figure 18 very closely generates the incoming, reflecting, and rereflecting stress waves observed in the experiment. The theoretical timings of these waves are well correlated, but with a small time lag generated by the initial zero magnitude of velocity and the NASTRAN three-point integration scheme. The initial zero velocity condition helps to produce a correct output velocity transient at the point of application.

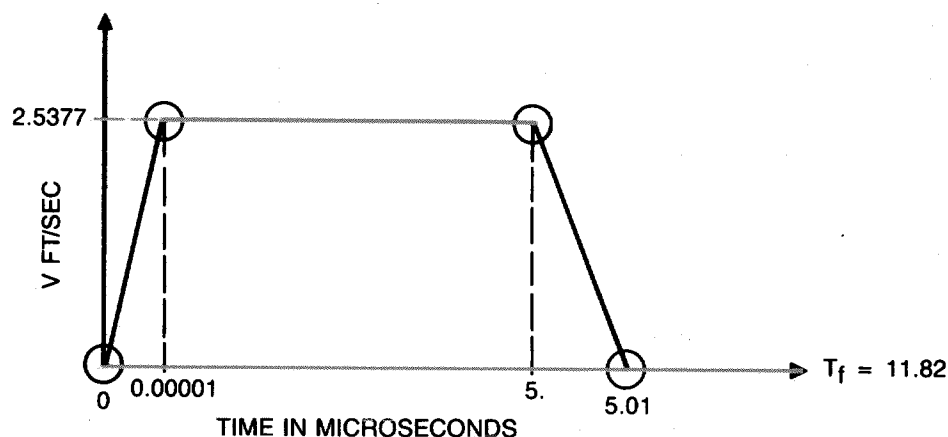


Figure 18. NASTRAN Input function.

4.2.4 Application of Constraints — Considering the input function of Figure 18, it is observed that the analysis time step, 0.01 microsecond, and the element size, 0.002 ft, are too stringent. Applying the constraints given in Section 3, the time step can be as high as 0.7 microsecond. The length of the rod element (0.0125 ft) is selected through the wave mechanics item (f) and the finite-element consideration for the vibrational modes of item (e). The NASTRAN run WAVE2E (Figure 19) uses this data and correctly duplicates the results of the run WAVE7R10. Differences in the graphs of Figures 17 and 19 are attributed to the amount of overshooting around the mean values explained in Section 4.1.2.1.

4.3 ELEMENT SIZE FOR SHOCK WAVE PROPAGATION

In this section an emphasis is on the selection of NASTRAN element size (L_e) for a shock of a given duration (t_p). Run SHOK5 and those of section 4.1 avoid this issue by generating a shock wave through initial condition (Equation 1). In the current study, the initial condition is removed. Keeping element size constant at 0.002 ft, shock duration t_p is varied to find the optimum value of n in the inequality of $L_e < t_p V_s/n$.

The analysis time step is 0.1 microsecond. This procedure is summarized in the following runs:

Run EDELT1 — This is a data generation run of SOL 69 with $t_p=1$ microsecond resulting in n of 8.4.

Run EDELT1A — This is a restart run of SOL 69 using the database created in EDELT1. It has $t_p=1$ microsecond, $n=8.4$. The run can generate, propagate and reflect the shock waves of the desired amplitudes. It is essential to locate a smaller value of n , if existing.

Run EDELT1B — This restart is for the shock duration $t_p=0.6$ microsecond, resulting in $n=5.08$. The data fails to generate rebounding wave of proper magnitude (Figure 20). Therefore, the optimum value of n is between 5 and 8.

Run EDELT1C — This is again a restart using a database created in RUN EDELT1. The run executes rigid format SOL 69 with $t_p=0.8$ microseconds and $n=6.7$. It has generated the optimum value of n , leading to the allowable finite-element length of item (f), Section 3. The stress transients at the free end (element 1), middle section (element 25) and the fixed end (element 50) are given in the graphs of Figures 21, 22, and 23.

In case of an oversized structure, one may perform an analysis of short duration on the fine mesh model and obtain the displacement transients at the boundaries. These transients then can be applied on the coarse mesh model for a long-duration analysis.

In some cases, the local zone of interest can be isolated from the large structure. It is then possible to perform a detailed analysis of the local area.

4.4 SELECTION OF PULSE DURATION t_p

Sometimes, the analyst may face a situation of selecting an appropriate value of pulse duration even for a given input shock function. The typical values are shown in Figure 24. The shock wave may have sharp peak reversals (stationary points) like the one depicted in Figure 24. The original curve, ACB, will be replaced by AA'B'B. The selection of t_p will follow the constraints of Section 3 with special care that t_p is not so unduly large as to affect the original shape. When there are multiple stationary points or plateaus, t_p should be the smallest of all the local magnitudes. The inequality (d) of Section 3 will produce a governing value.

Since the NASTRAN numerical scheme has a tendency to reduce the magnitude at an attempted stationary value, the input curve AA'B'B will try to trace, in reality, the ACB section. Some of the hydro-

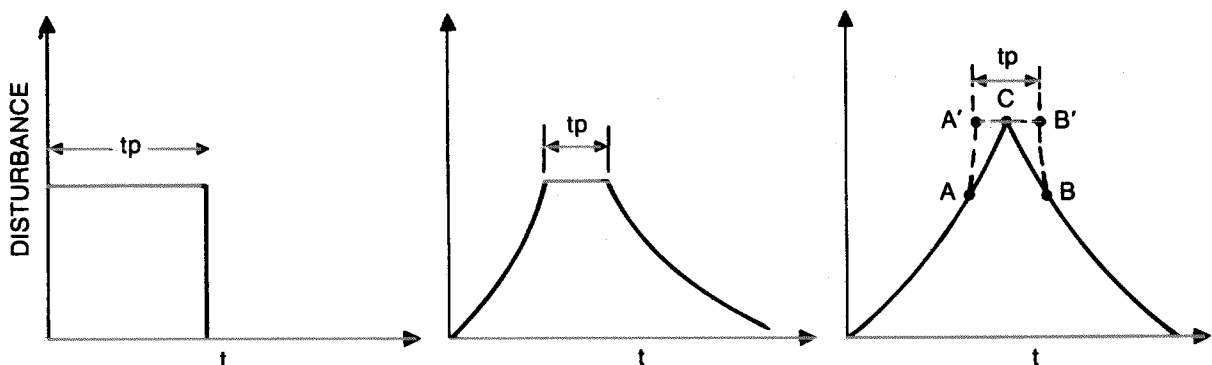


Figure 24. Suggested t_p values of input shock functions.

codes (e.g., PISCES) preserve the shape of the input pulse because of their explicit theoretical formulations and the existence of higher-order terms in the analysis.

5. CONCLUSIONS

This study covers the usage of NASTRAN to explain the shock wave propagation through solids. The phenomenon under consideration is strictly for the linear analytical conditions. The NASTRAN results, correlating with the wave mechanics mathematical formulation and the experimental observations, lead to the following conclusions:

- A. Numerical methods employed in NASTRAN linear algorithms (SOL 27, 69, 31, and 72) are acceptable even under very small analysis time steps (e.g. 0.01 microsecond) and element sizes (e.g. 0.002 ft).
- B. The semiempirical rules for the selection of NASTRAN input parameters listed in Section 3 can be successfully used to analyze shock wave propagation through solids.
- C. Finite-element or similar discretization models tend to overshoot the stress transients around the mean values. A proper interpretation of the graphs is essential. (Section 4.1.2.1).
- D. In general, the variable time steps and the restart capabilities of NASTRAN help to save the computer run time (CPU) considerably. This is particularly true in the environment of shock wave propagation. (Sections 4.1.2.5 and 4.2.2).
- E. When the structure is subjected to a sudden shock followed by a slow transient, the former generates the initial conditions of the latter analysis (e.g. blast waves, dynamic buckling, shaped charge, etc). It is essential that the shock wave analysis should produce proper displacement, velocity, and acceleration time-histories (Section 4.2.3).
- F. The shock wave analysis results are sensitive to the input parameters of NASTRAN. There exists a high probability of generating logical errors involving a wrong output of generalized forces and displacements, unless proper input constraints are imposed.

ACKNOWLEDGEMENTS

The author acknowledges the useful suggestions of Hugh McCutchen and the encouragement from the management of General Dynamics Space Systems Division, Erich Wolf, Lee Browning, John Wohlwend, and Gene Perkins.

REFERENCES

1. Y.C. Fung, *Foundations of Solid mechanics*, Prentice-Hall, Inc., 1975.
2. H. McCallion, *Vibration of Linear Mechanical Systems*, John Wiley & Sons, 1973.
3. D.J. Hatter, *Matrix Computer Methods of Vibration Analysis*, John Wiley & Sons, 1973.
4. John M. Biggs, *Structural Dynamics*, McGraw-Hill Co., 1964.
5. R.D. Cook, *Concepts and Applications of Finite Element Analysis*, John Wiley & Sons, 1974.
6. M.M. Moharir, *NASTRAN Nonlinear Capabilities in Dynamic Solutions*, MSC/NASTRAN User's Conference Proceedings, March, 1985.

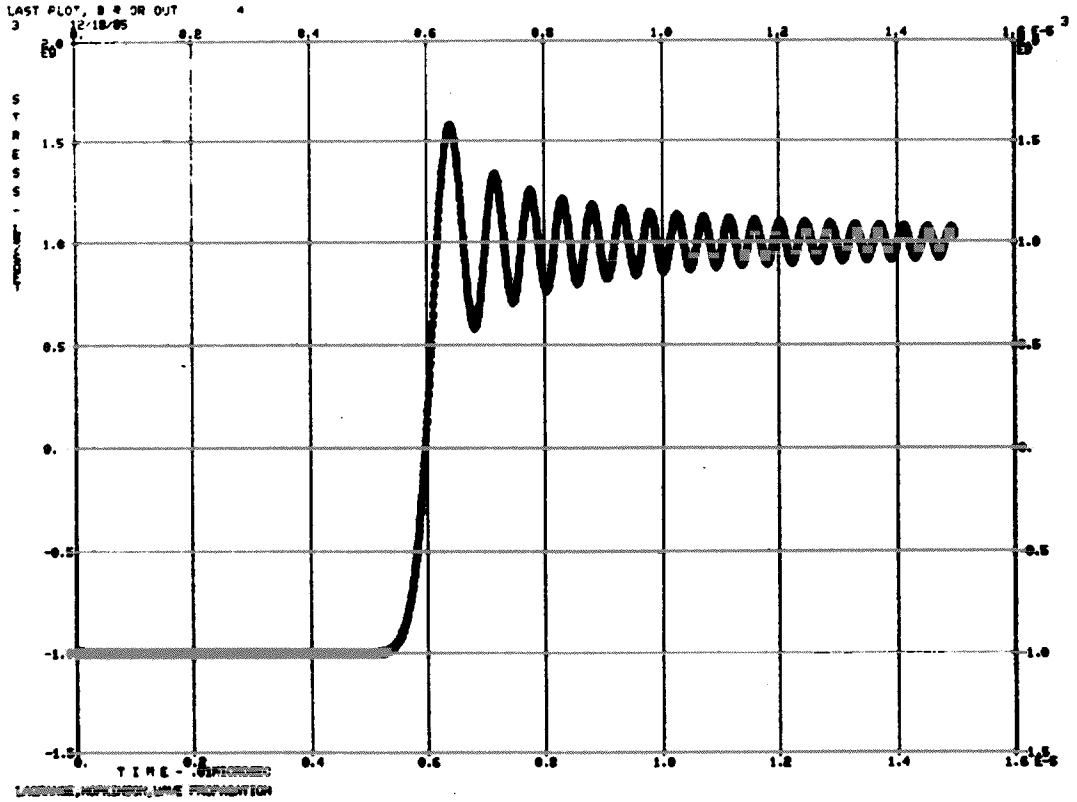


Figure 3. Stress time-history, Element 50, Run SH0K6.

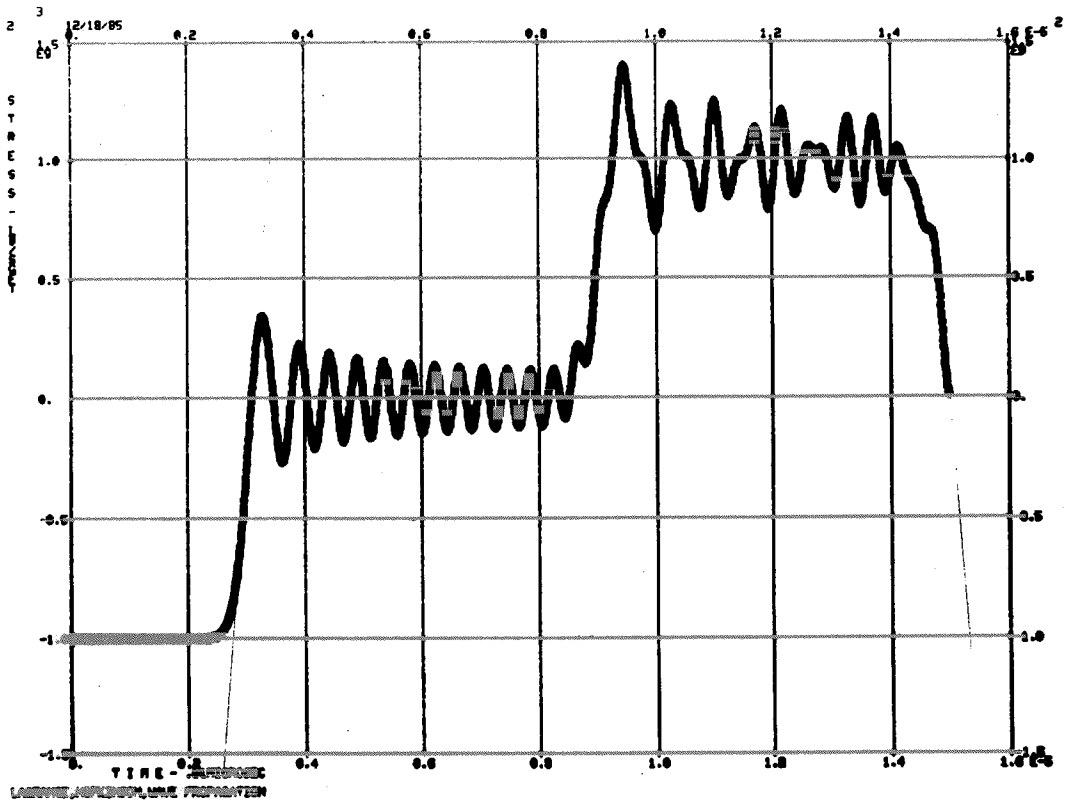


Figure 4. Stress time-history, Element 25, Run SH0K6.

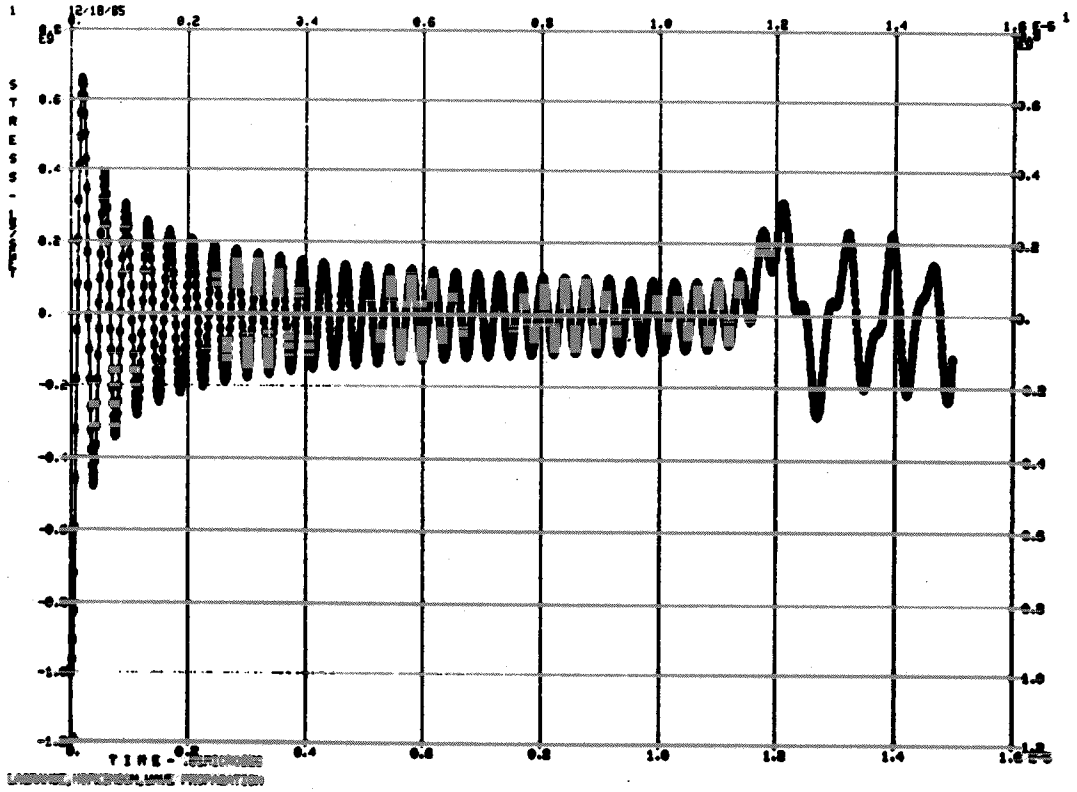


Figure 5. Stress time-history, Element 1, Run SHOK6.

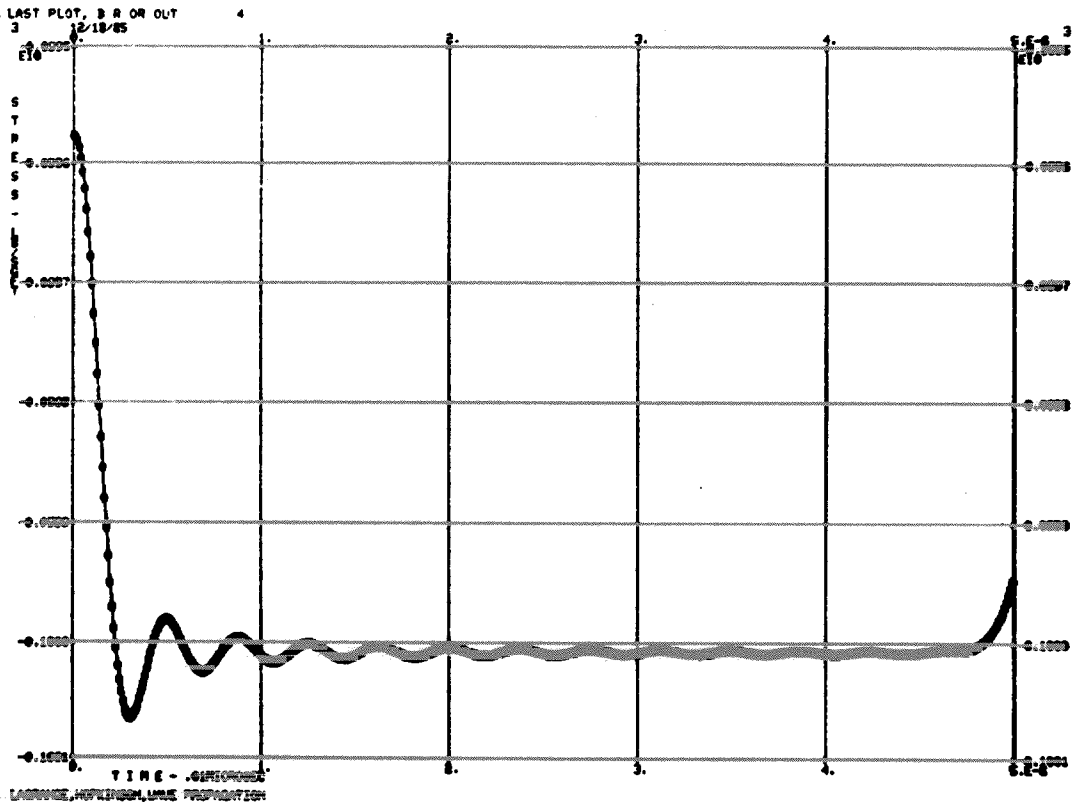


Figure 6. Stress time-history, Element 50, Run SHOK5.

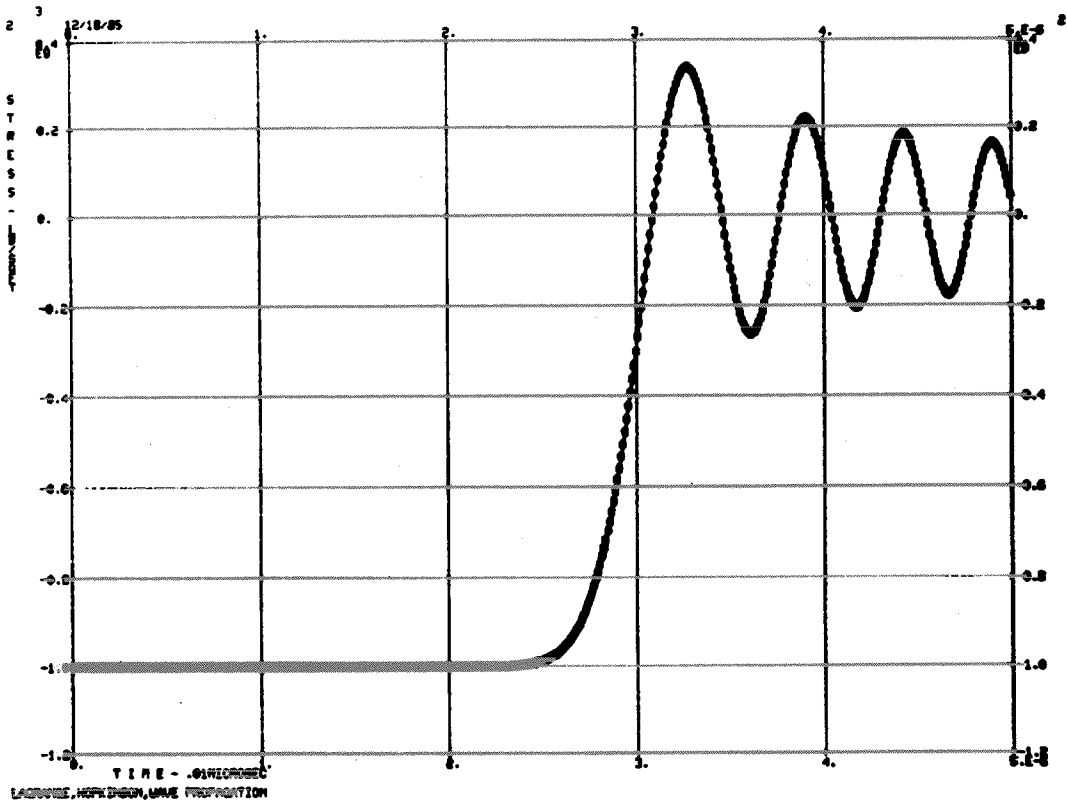


Figure 7. Stress time-history, Element 25, Run SHOK5.

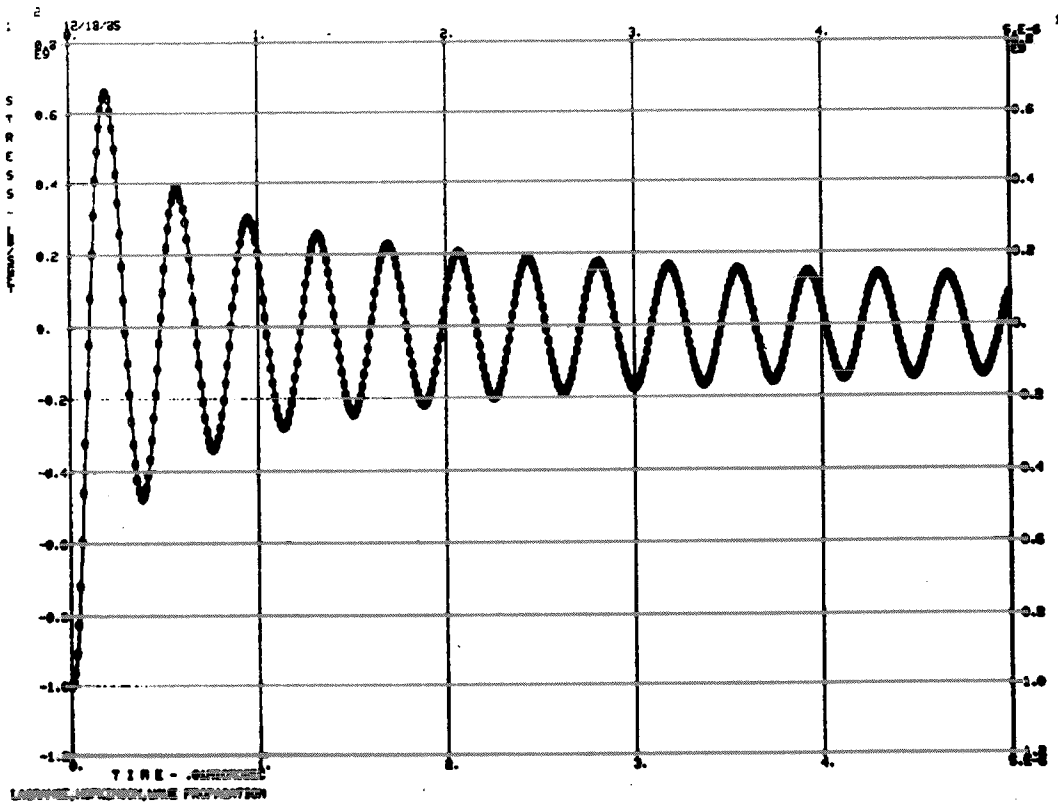


Figure 8. Element time-history, Element 1, Run SHOK5.

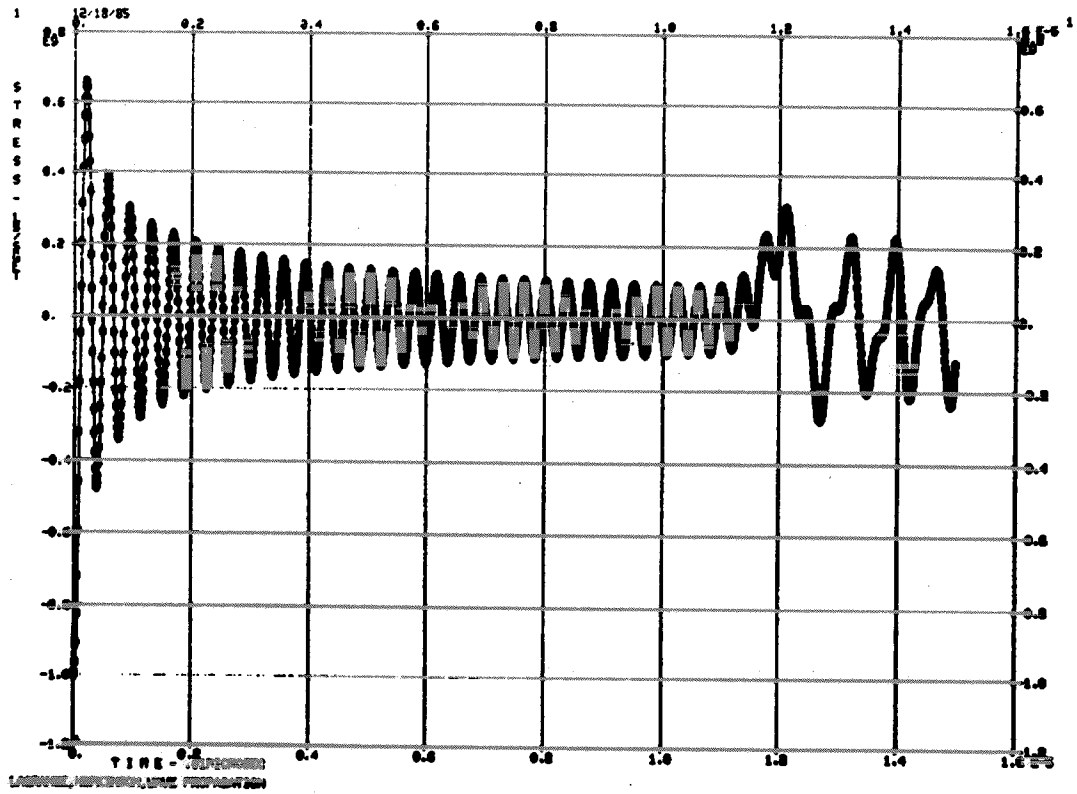


Figure 5. Stress time-history, Element 1, Run SHOK6.

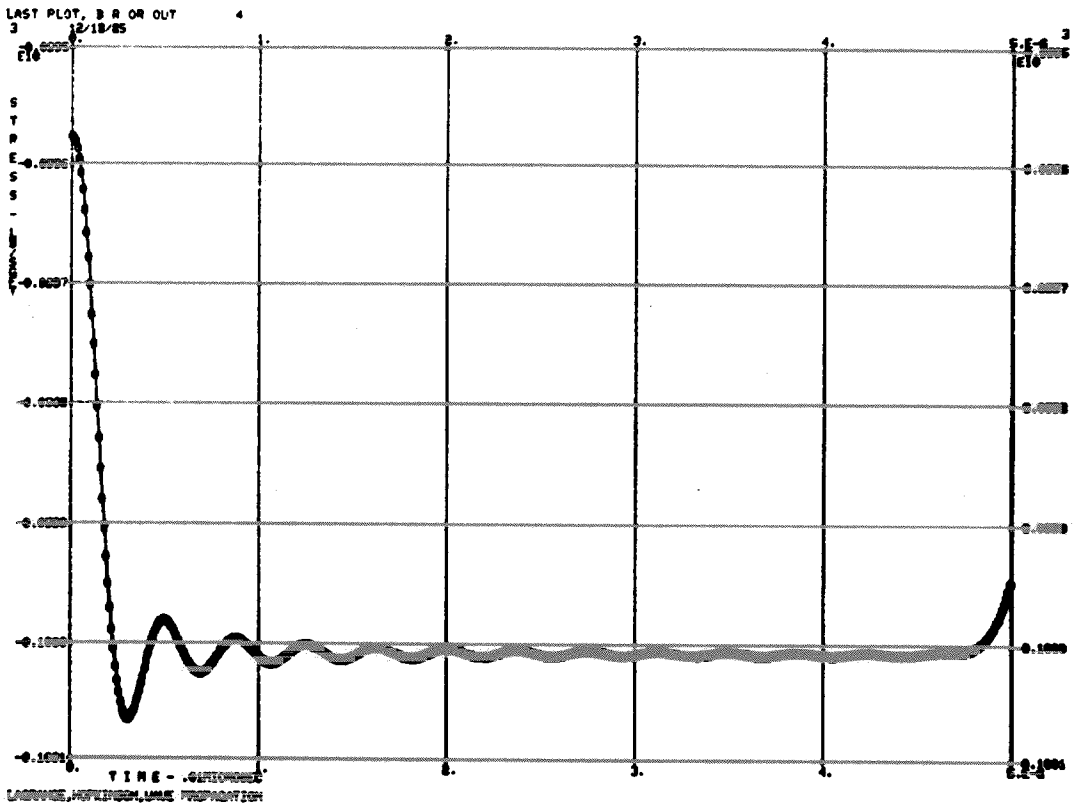


Figure 6. Stress time-history, Element 50, Run SHOK5.

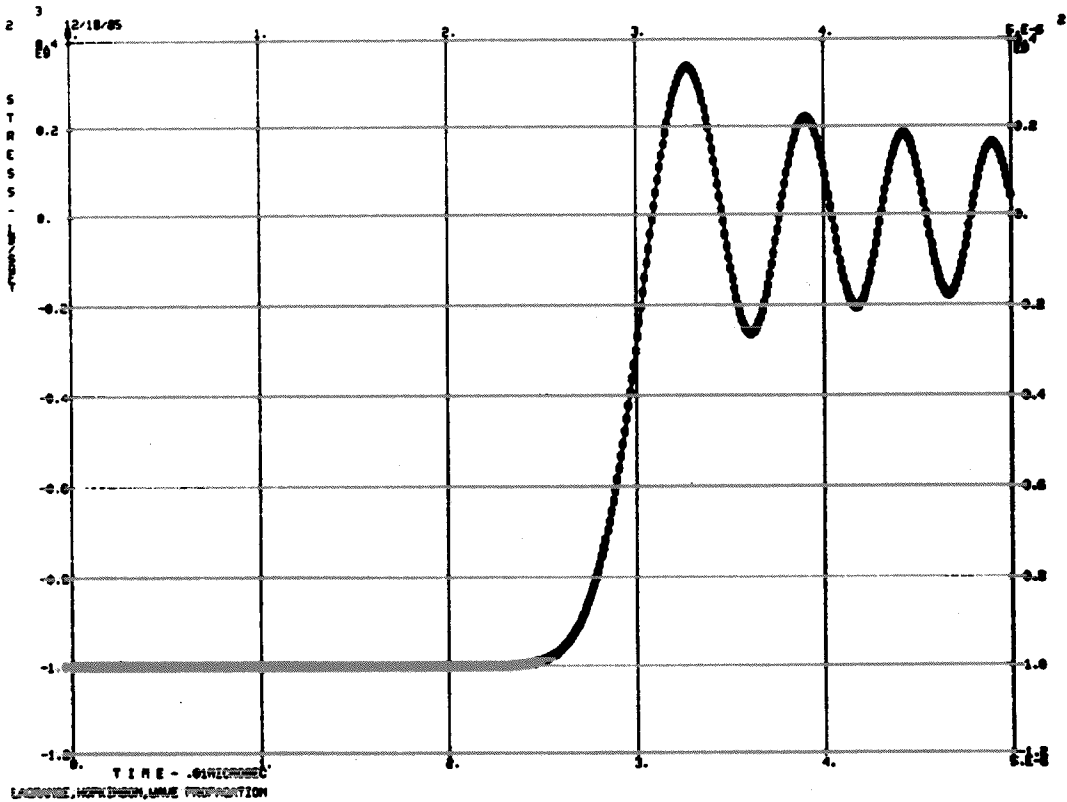


Figure 7. Stress time-history, Element 25, Run SHOK5.

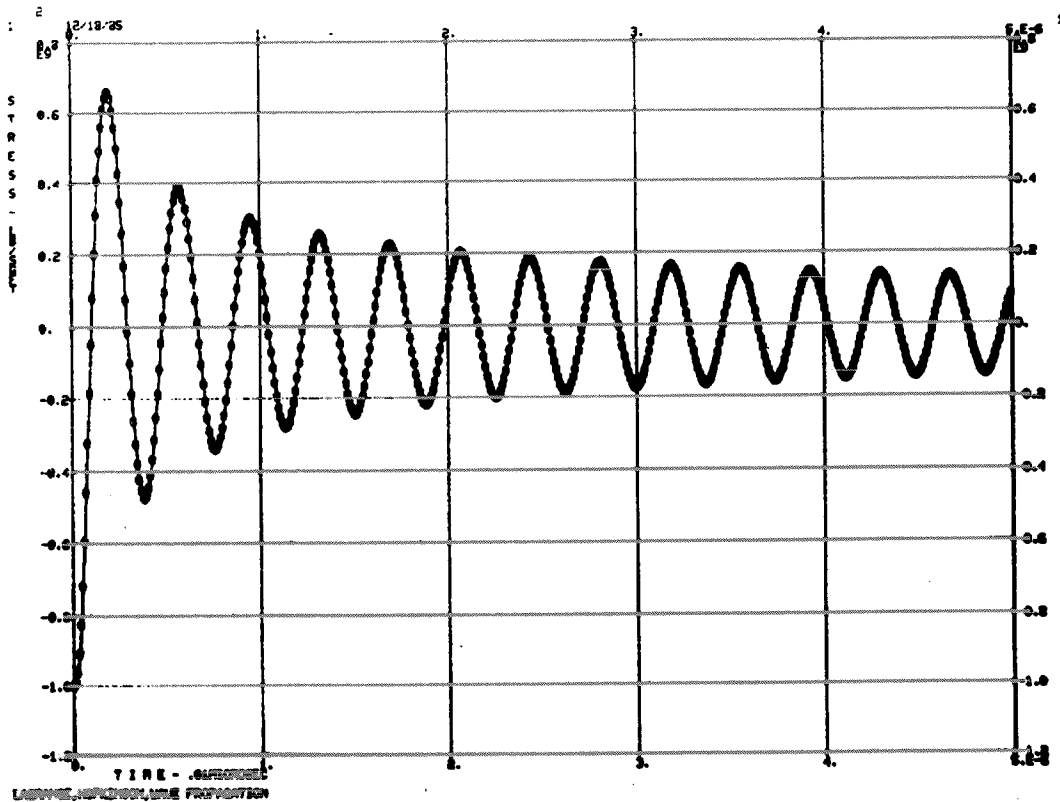


Figure 8. Element time-history, Element 1, Run SHOK5.

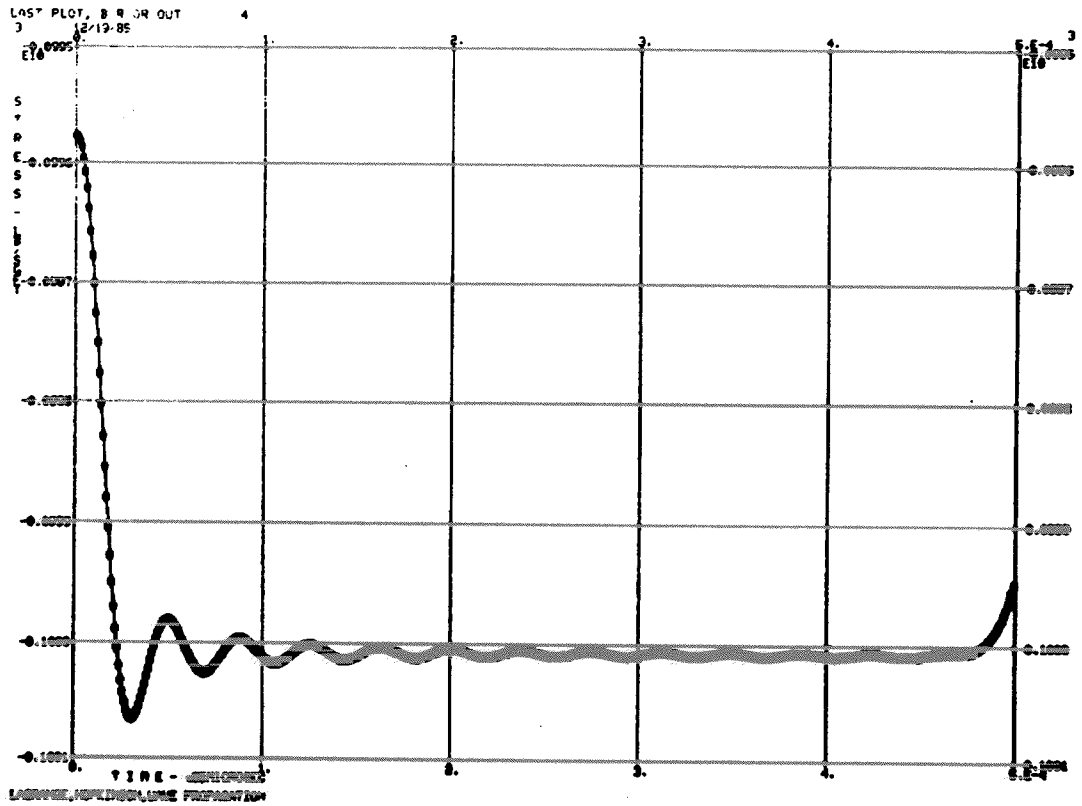


Figure 9. Stress time-history, Element 50, Run SH0L5.

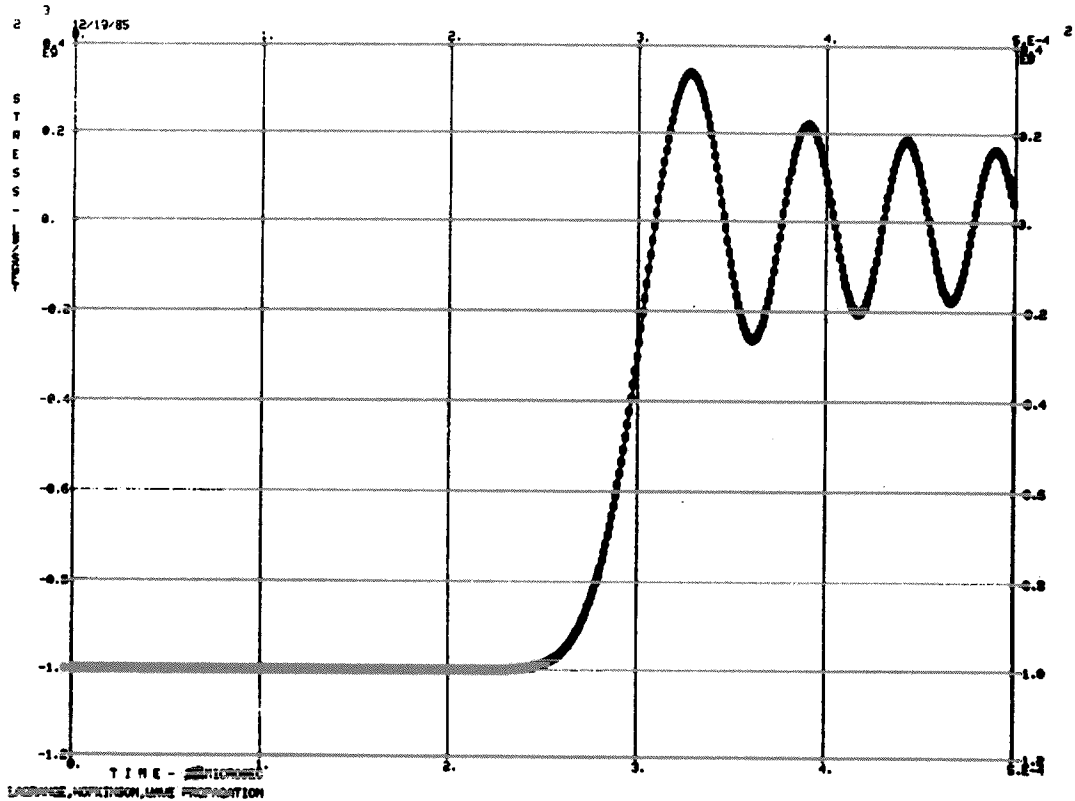


Figure 10. Stress time-history, Element 25, Run SH0L5.

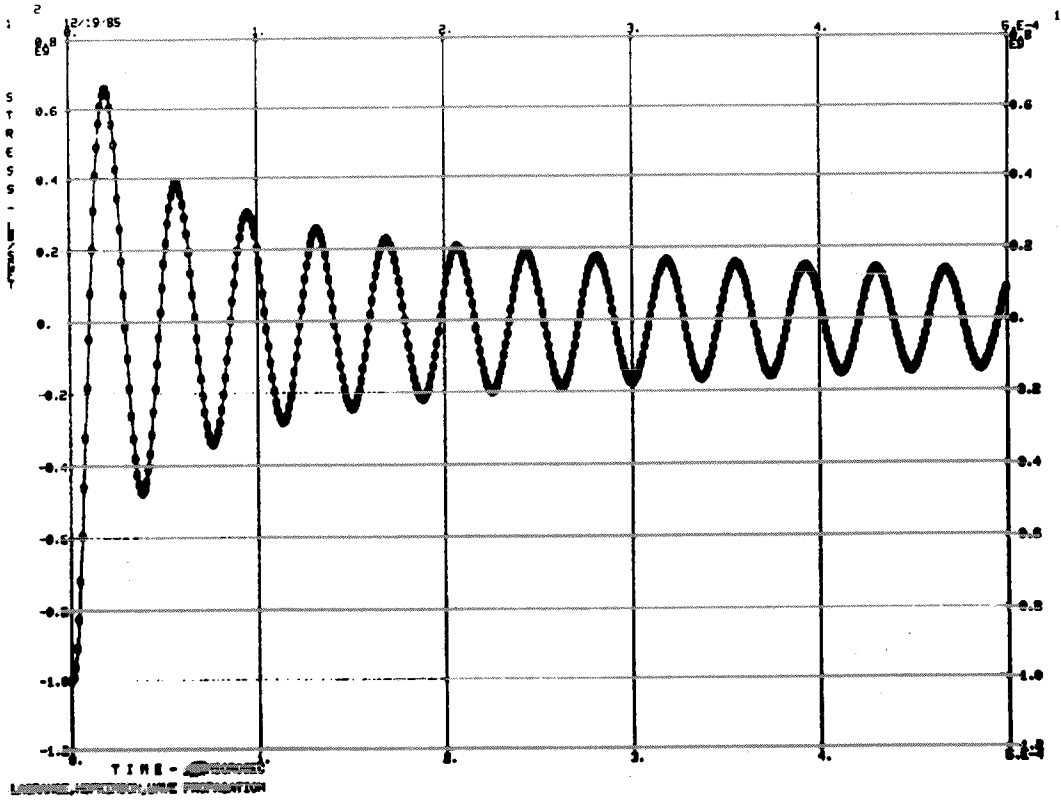


Figure 11. Stress time-history, Element 1, Run SH0L5.

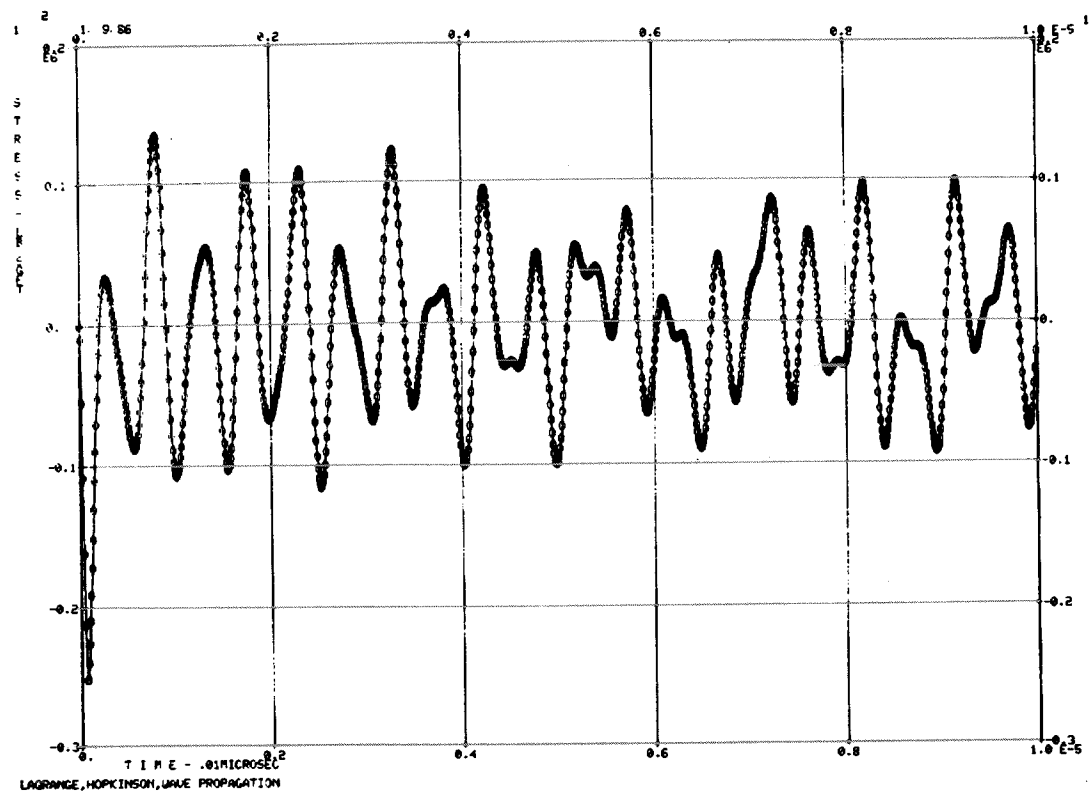


Figure 13. Stress time-history, Element 1, Run WAVE7R5.

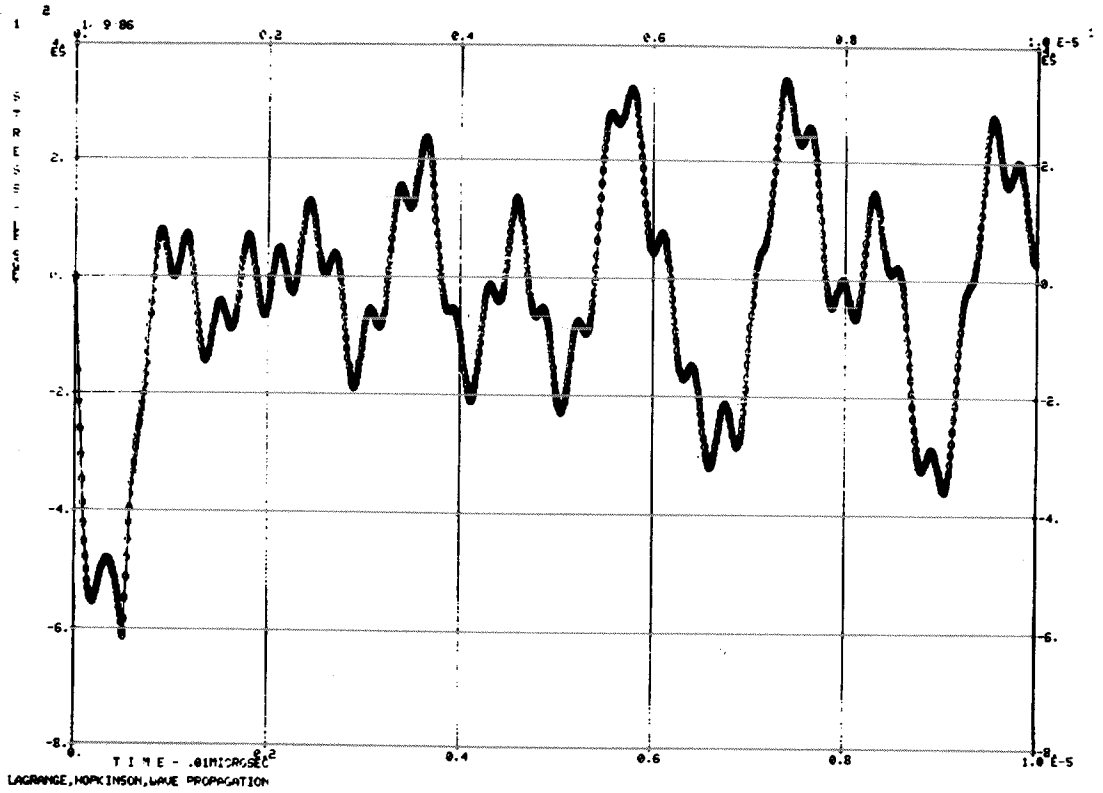


Figure 14. Stress time-history, Element 1, Run WAVE7R6.

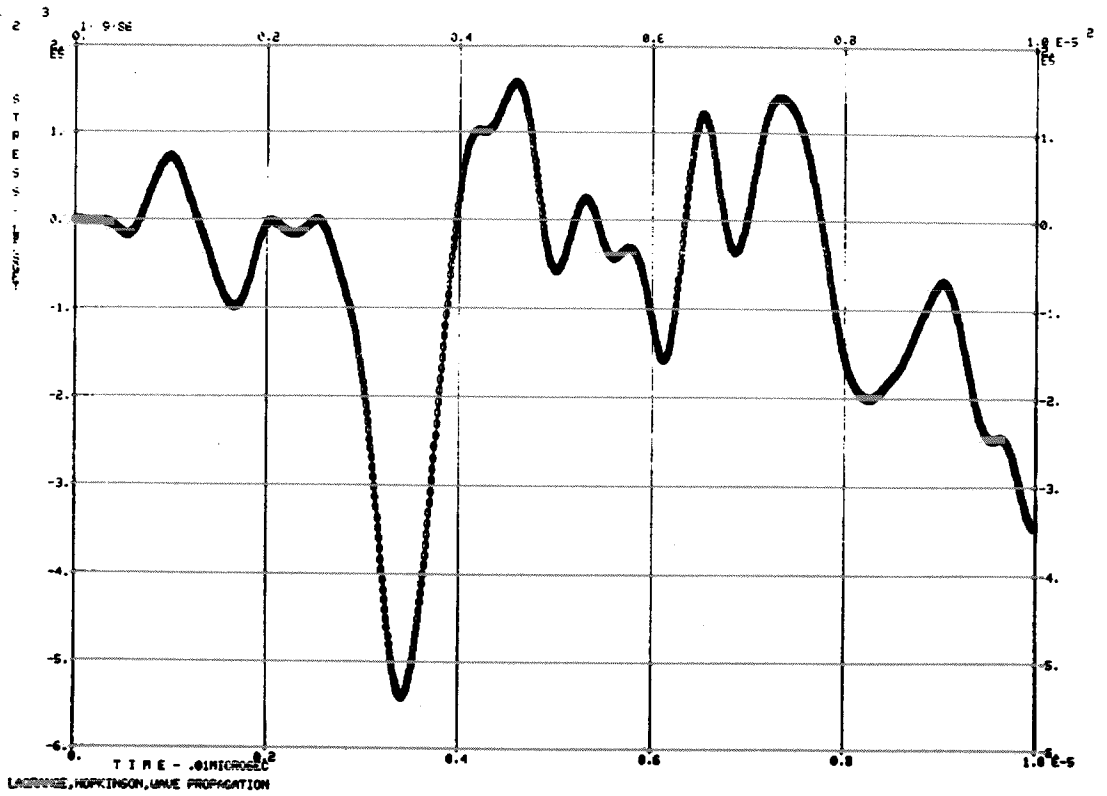


Figure 15. Stress time-history, Element 25, Run WAVE7R6.

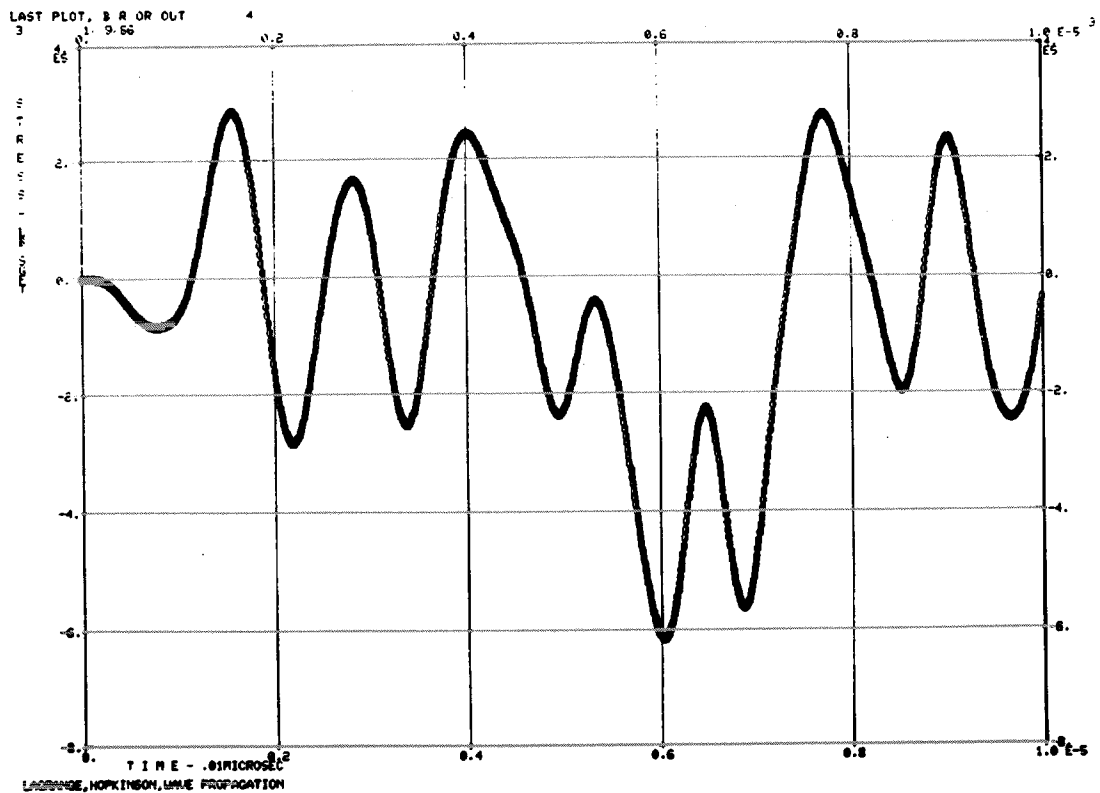


Figure 16. Stress time-history, Element 50, Run WAVE7R6.

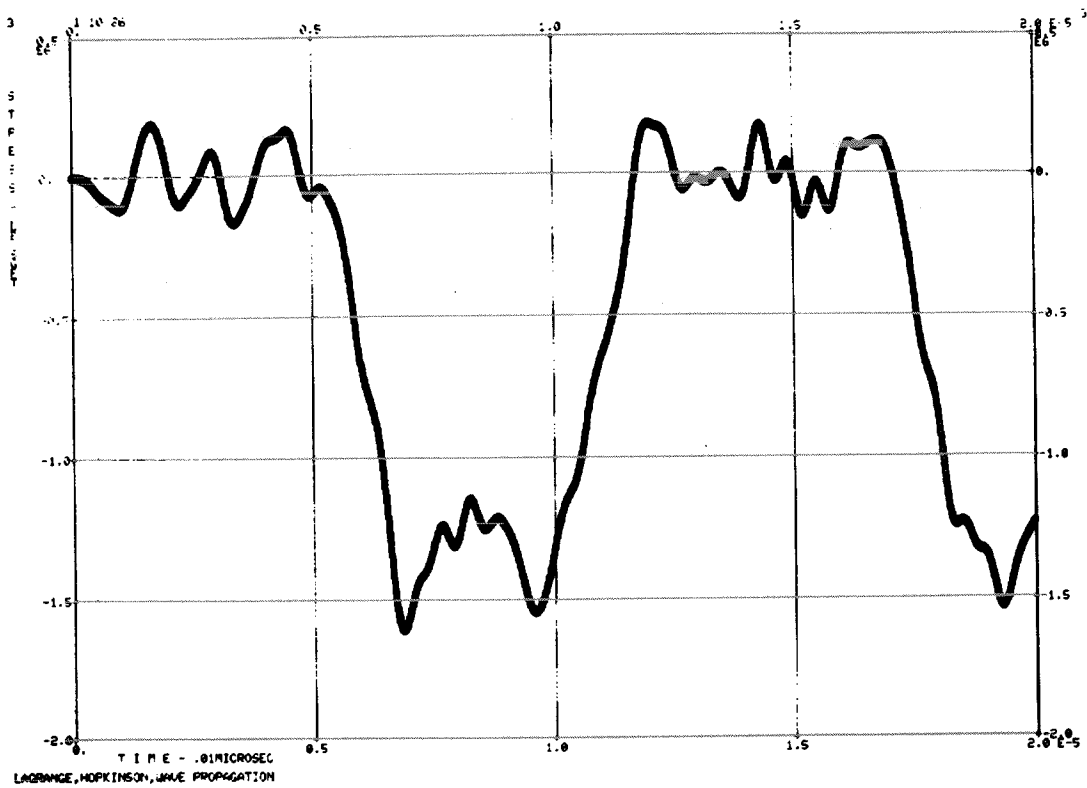


Figure 17. Stress time-history, Element 50, Run WAVE7R10.

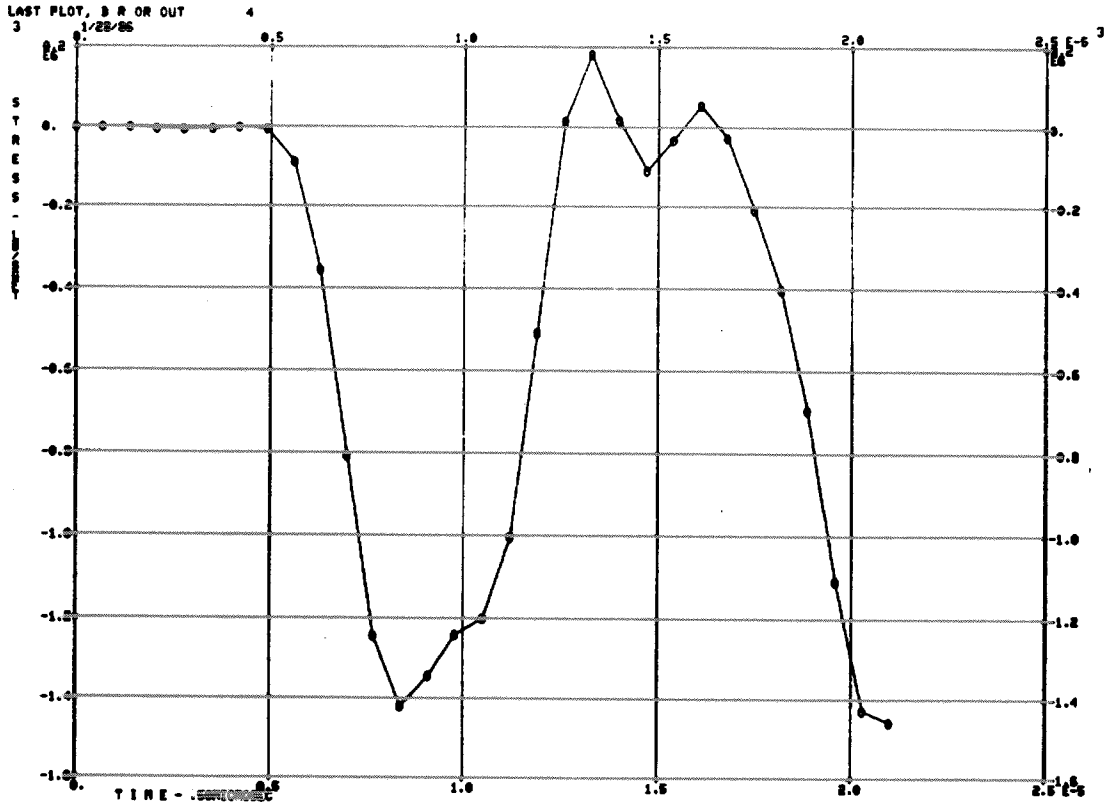


Figure 19. Stress time-history, Element 8, Run WAVE2E.

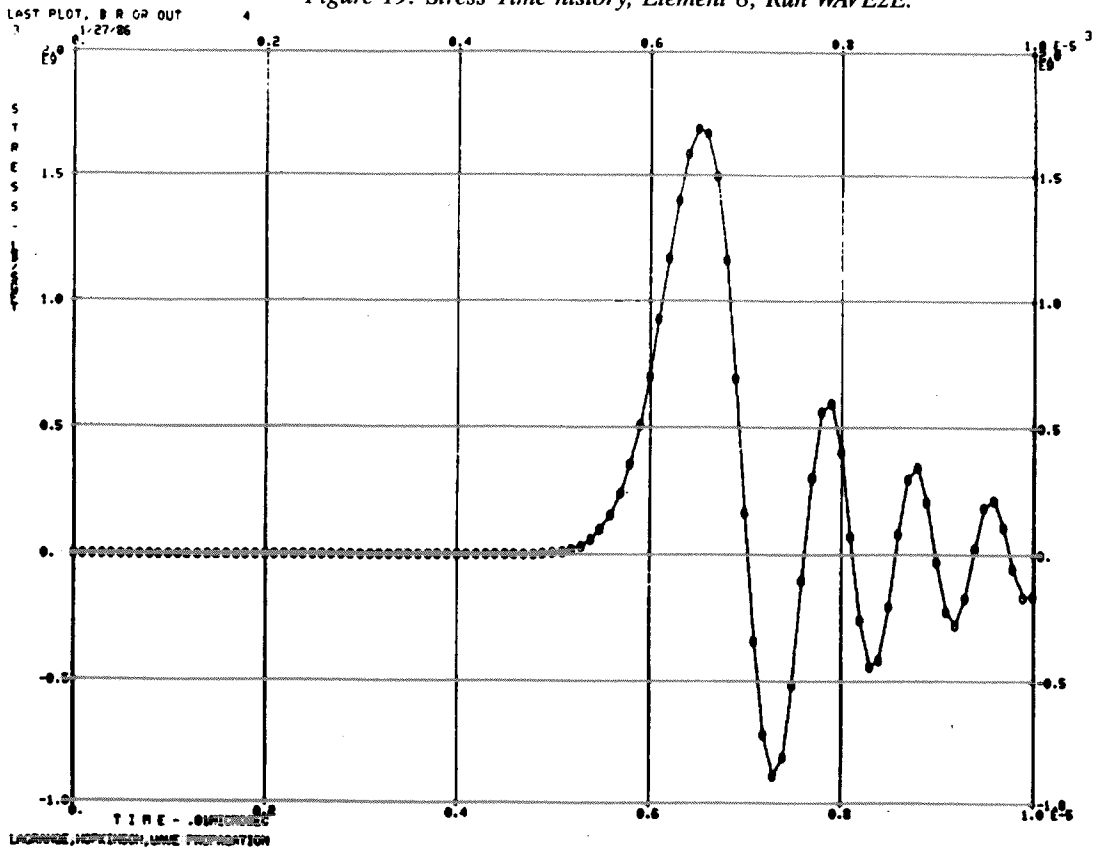
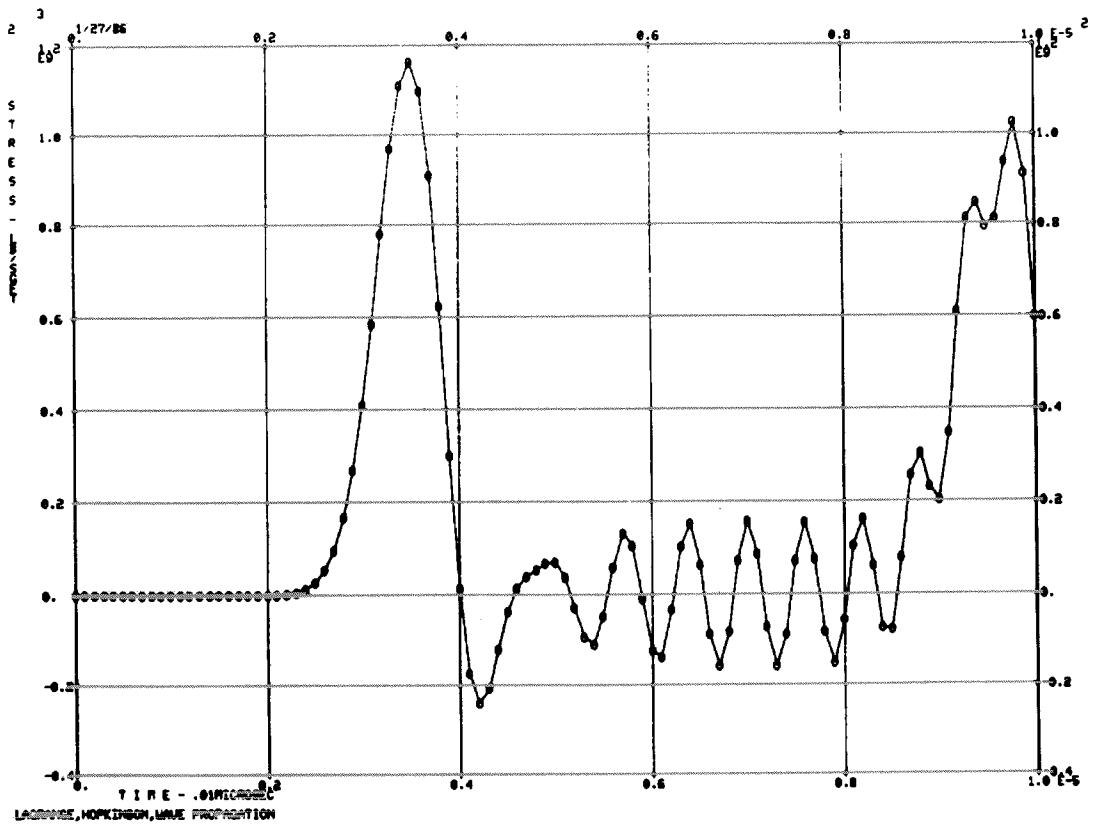
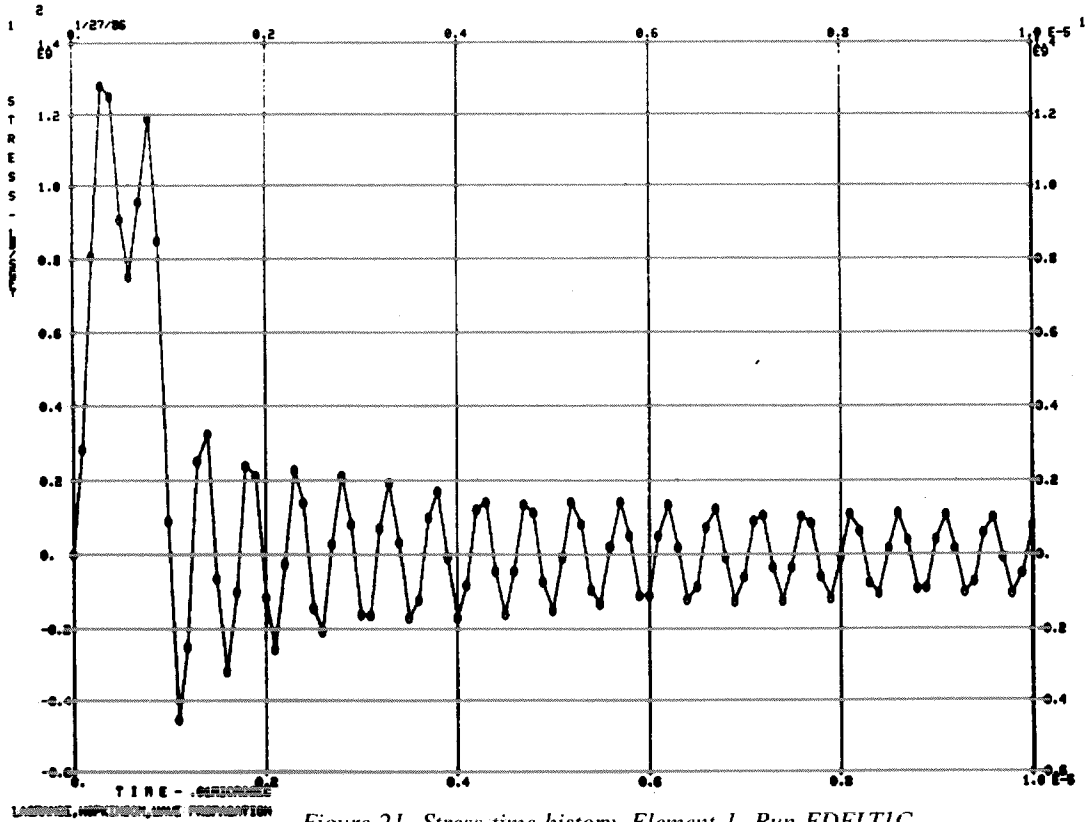


Figure 20. Stress time-history, Element 50, Run EDELT1B.



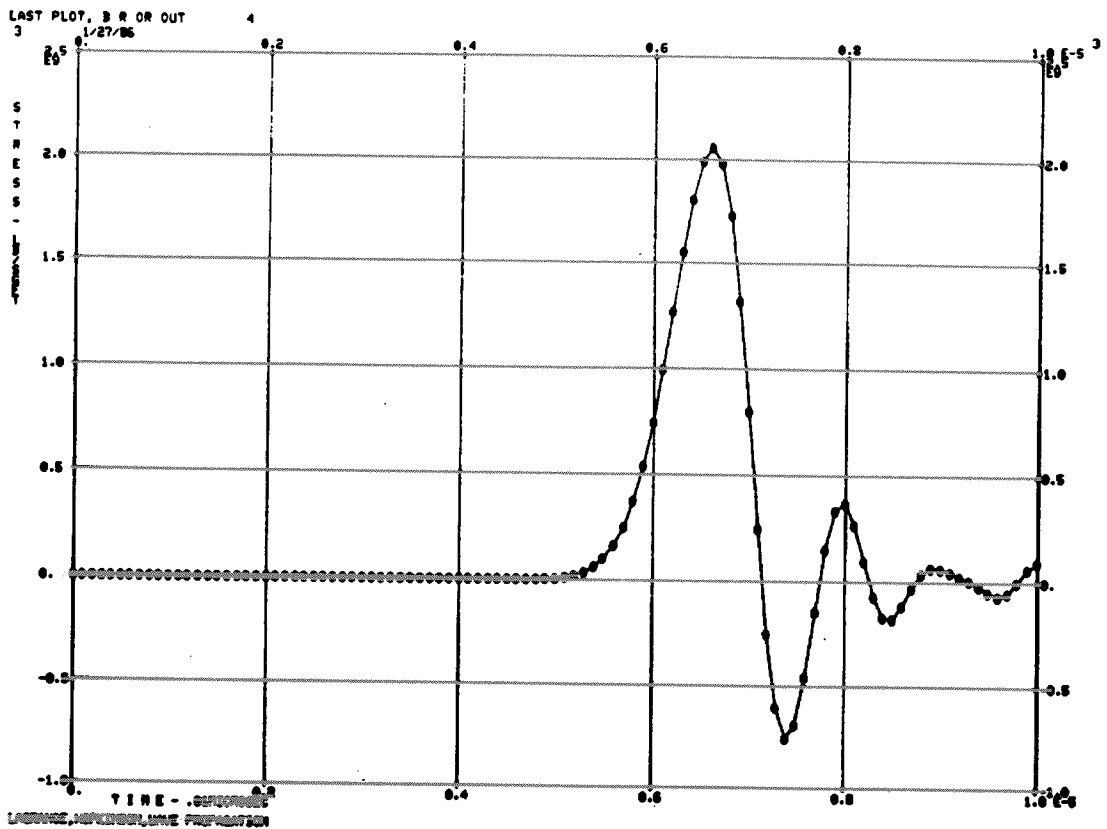


Figure 23. Stress time-history, Element 50, Run EDELTC.